THE JOURNAL OF PHYSICAL CHEMISTRY A

Article

pubs.acs.org/JPCA

Atomic Resolution for the Energy Derivatives on the Reaction Path

Mateusz Jędrzejewski,[†] Piotr Ordon,[‡] and Ludwik Komorowski*[,†]

[†]Department of Physical and Quantum Chemistry, Wrocław University of Technology, Wyb. Wyspiańskiego 27, 50-370 Wrocław, Poland

[‡]Department of Physics and Biophysics, Wrocław University of Environmental and Life Sciences, ul. Norwida 25, 50-373 Wrocław, Poland

ABSTRACT: Definite algorithms for calculation of the atomic contributions to the reaction force F_ξ and the reaction force constant k_ξ (the first and the second derivatives of the energy over the reaction path step) are presented. The electronic part in the atomic and group contributions has been separated, and this opened the way to identification of the reactive molecule fragments on the consecutive stages of the reaction path. Properties have been studied for the two canonical test reactions: CO + HF → HCOF and HONS → ONSH.

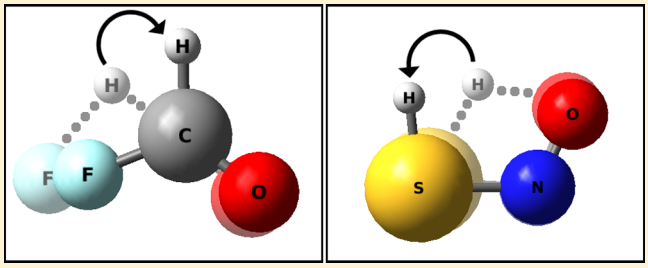

1. INTRODUCTION

The concept of the reaction force F_ξ (first derivative of the energy over the reaction progress ξ) introduced by Toro-Labbé and coworkers[1−5] opened a promising field of exploration for the theoretical and computational studies of chemical reactions. Jaque, Politzer, and coworkers also first analyzed the second energy derivative (k_ξ), which they adequately called the reaction force constant.[6,7] The concept found interesting applications as an indicator of synchronicity in some reactions.[8,9]

Subsequent studies of a great deal of the reactions led to the general suggestions endorsed by the main authors[10,11] that physically meaningful stages of the reaction process can be identified by the mathematically characteristic points on the $E(\xi)$ relationship: the preparation phase of geometry being modified, the new bond formation process, and the similar two-step relaxation to the new energy minimum. It has not been claimed that the different regions feature exclusively structural or electronic effects; nevertheless, the authors tend to distinguish[12] "the initial and final regions as those manifesting the identities of the reactant(s) and products(s), respectively", with the border lines fixed at the maximum reaction force points (zero reaction force constant).

The specific feature of the method applied by the pioneering authors was the analysis of the energy of the whole reactive supermolecule system on the reaction path. This approach, very appropriate for small reacting molecules, loses its power when applied to the systems, where only a side chain or distant fragment is affected by the actual reaction, leaving the rest of the system intact. In two recent publications the efforts have been demonstrated to bring the global description closer to the chemical reality by exposing the role of individual atoms. Inostroza-Rivera et al.[13] calculated the atomic contributions to the total energy of the system using the energy decomposition scheme, based on the procedure developed by Pendas et al.,[14] to compute the two-electron integrals over arbitrary regions of space, thus relating their work to the AIM atoms. The authors explored their own approximation in adopting the sophisticated scheme to the DFT calculations. A more direct approach has previously been tested by Vöhringer-Martinez and Toro-Labbe.[15] They have calculated the contributions to the activation energy from each atom in the system. For the proton transfer reaction in HONS, the authors merely noticed the dominant role of proton but would not search for the variable role of each atom in the reaction stages.

This observation led the present authors to the idea of broadening the concept of the reaction force and the reaction force constant by identifying the contributions to those from individual atoms. The atoms can be identified by their nuclei and thus with no need to apply any arbitrary partition scheme for the electron density. In contrast with the energy itself, partitioning of its derivatives into atoms can be achieved directly.

The foundations of the presented method rest on the work by Ordon and Komorowski[16,17] focused on the analysis of the energy derivatives within the conceptual DFT analysis and the vibrational softening of molecules.[18−21] The important DFT sensitivity indices (nuclear reactivity and nuclear stiffness) have been proposed for bonded atoms, exploring the Hellman−Feynman forces acting on the nuclei of atoms forming a molecular entity. The authors demonstrated how the readily computed H−F forces on the nuclei can be explored in mapping the properties of the density, very much in line with the basic Hohenberg & Kohn theorem.[22] Combining this concept with the well-established computational scheme for the IRC has opened the field of the analysis.

Two simple reaction systems have been selected to test the approach. The reaction HF+CO → HCOF was formerly studied

Received: April 4, 2016
Revised: May 16, 2016
Published: May 17, 2016

DOI: 10.1021/acs.jpca.6b03408
J. Phys. Chem. A 2016, 120, 3780−3787

by Ordon et al.[23−25] investigating the electronic hardness and electron dipole polarizability variation on the reaction path. The proton migration reaction HONS → ONSH was studied by several authors within the reaction force formalism.[26−29] This simple reaction has offered the particular opportunity to further developed the virial approach already applied to this system.[15] The common feature of both selected reactions is their regional character within rather small systems of atoms: the group CO in the first and the ONS group in the second reaction seem to be merely spectators to the reaction run because their geometry is hardy affected. Thus, the atomic contributions to the energy derivatives are expected to demonstrate a much different role of atoms in the reaction run.

2. METHODS

Resolution of the Reaction Force to Atoms. The reaction force has originally been proposed as the scalar property to characterize the reaction mechanism by using the reaction progress coordinate as a variable. It is the textbook defined scalar parameter,[30] ξ, that is the step measure along the IRC.[31,32] In some later studies, though, the authors have chosen to discuss the ill-defined vector coordinate, $\mathbf{R}_c$, instead,[10,11,33] with the reaction force appearing to be a vector; this, however, has never been shown in a numerical work. In this present analysis, the tradition of the original concept is followed.

The Hellman−Feynman force acting on the nucleus uniquely identifies a nucleus A in molecule M

$$\mathbf{F}_{A\in M} \equiv -\left(\frac{\partial E_M}{\partial \mathbf{R}_A}\right) \quad \text{or} \quad F_{i,A} = -\frac{\partial E_M}{\partial R_{A,i}} (i = x, y, z \in A) \tag{1}$$

The reaction force on each step of the IRC can thus be decomposed into contributions from atoms by directly introducing the H−F forces $\mathbf{F}_A$ on each nucleus

$$F_\xi = -\frac{\mathrm{d}E_M}{\mathrm{d}\xi} = -\sum_{A\in M} \frac{\partial E_M}{\partial \mathbf{R}_A}\cdot\frac{\mathrm{d}\mathbf{R}_A}{\mathrm{d}\xi} = \sum_{A\in M} \mathbf{F}_A\cdot\frac{\mathrm{d}\mathbf{R}_A}{\mathrm{d}\xi} = \sum_A F_A(\xi) \tag{2}$$

Here the vector $\mathrm{d}\mathbf{R}_A/\mathrm{d}\xi$ stands for the virtual change in the position of nucleus on that particular step. The contribution of an atom to the reaction force (a number) is represented by the scalar product of two vectors

$$F_A(\xi) = \mathbf{F}_A\cdot\frac{\mathrm{d}\mathbf{R}_A}{\mathrm{d}\xi} = -\frac{\partial E_M}{\partial \mathbf{R}_A}\cdot\frac{\mathrm{d}\mathbf{R}_A}{\mathrm{d}\xi} = \sum_{i\in A}^{x,y,z} F_{A,i}\cdot\frac{\mathrm{d}R_{A,i}}{\mathrm{d}\xi} \tag{3}$$

Because $F_A(\xi)$ are additive (eq 2), the summation may also be extended to fragments composed from several atoms, for example

$$F_{ABC}(\xi) = F_A(\xi) + F_B(\xi) + F_C(\xi) \tag{4}$$

The very definition of the scalar $F_A(\xi)$ (eq 3) makes it independent of the computational rigor (Cartesian or mass-weighted coordinates). The atomic or reasonably chosen group contributions to the reaction force may contain the effect of magnitude of forces acting on the nucleus and the effect of its virtual displacement; both factors are variable as the reaction proceeds.

Atomic Contributions to the Reaction Force Constant. Because F_ξ is given independently as the energy derivative (eq 2), it is also possible to trace the second energy derivative over the reaction progress; the reaction force constant $k_\xi = -\mathrm{d}F_\xi/\mathrm{d}\xi$ (the convention originally proposed[8,9]). By repeating the scheme of eq 2 we have

$$k_\xi = -\frac{\mathrm{d}F_\xi}{\mathrm{d}\xi} = -\sum_A \frac{\mathrm{d}F_A(\xi)}{\mathrm{d}\xi} = -\sum_A \frac{\mathrm{d}}{\mathrm{d}\xi}\left[\mathbf{F}_A\cdot\frac{\mathrm{d}\mathbf{R}_A}{\mathrm{d}\xi}\right] = \sum_A k_A(\xi) \tag{5}$$

The final summation in eq 5 is over all atoms. The individual contribution from an atom can be calculated using the result for $F_A(\xi)$ in eq 3. Equation 5 proves that definite partition of k_ξ into the contributions from each coordinate is possible; hence the reaction force constant k_ξ may also be additively composed from atomic contributions. Because of the computational rigor of the IRC, the atomic displacements $\Delta\mathbf{R}_A(\xi)$ calculated on each step are all straight lines parallel to the acting forces $\mathbf{F}_A$. As consequence, the second derivatives $\mathrm{d}^2\mathbf{R}_A/\mathrm{d}\xi^2$ vanish on each step, and the atomic contribution to the reaction force constant becomes simply a scalar product of two vectors

$$k_A(\xi) = -\frac{\mathrm{d}F_A(\xi)}{\mathrm{d}\xi} = -\frac{\mathrm{d}\mathbf{F}_A}{\mathrm{d}\xi}\cdot\frac{\mathrm{d}\mathbf{R}_A}{\mathrm{d}\xi} \tag{6}$$

The displacement vector derivatives $\mathrm{d}\mathbf{R}_A/\mathrm{d}\xi$ are readily available from the geometry of the system on each step. The force derivative $\mathrm{d}\mathbf{F}_A/\mathrm{d}\xi$ in eq 6 can be eliminated by exploring the Cartesians force constants k_{ij} in the Hessian for the structure on each step of the IRC.

$$\frac{\mathrm{d}F_{A,i}}{\mathrm{d}\xi} = \sum_j^{3N} \frac{\mathrm{d}F_{A,i}}{\mathrm{d}R_j}\frac{\mathrm{d}R_j}{\mathrm{d}\xi} = \sum_j^{3N} k_{ij}\frac{\mathrm{d}R_j}{\mathrm{d}\xi} \tag{7}$$

$R_j \in [x_1, y_1, z_1, x_2 y_2, z_2, \ldots]$ are the coordinates of the $\mathbf{R}_A$ vectors. According to the Wilson convention,[34] the derivatives of forces are simply the Cartesian force constants: $\frac{\mathrm{d}F_i}{\mathrm{d}R_j} = k_{ij} = k_{ji}$. Consequently, the atomic contribution to the reaction force constant reads (eq 6)

$$k_A(\xi) = \sum_{i\in A}^{x,y,z} k_i(\xi) = -\sum_{i\in A}^{x,y,z} \frac{\mathrm{d}R_{A,i}}{\mathrm{d}\xi}\sum_j^{3N} k_{ij}\frac{\mathrm{d}R_j}{\mathrm{d}\xi} \tag{8}$$

The terms involving atom A only may be exposed in this expression

$$k_A(\xi) = -\sum_{i\in A}^{x,y,z}\sum_{j\in A}^{x,y,z} k_{ij}\frac{\mathrm{d}R_j}{\mathrm{d}\xi}\frac{\mathrm{d}R_i}{\mathrm{d}\xi} - \sum_{i\in A}^{x,y,z}\sum_{B\neq A}^{N}\sum_{j\in B}^{x,y,z} k_{ij}\frac{\mathrm{d}R_j}{\mathrm{d}\xi}\frac{\mathrm{d}R_i}{\mathrm{d}\xi} \tag{9}$$

Hence, eq 9 becomes a sum of the self-term $k_{AA}(\xi)$ and the effect of neighboring atoms $k_{AB}(\xi)$

$$k_{AA}(\xi) = -\sum_{i\in A}^{x,y,z}\sum_{j\in A}^{x,y,z} k_{ij}\frac{\mathrm{d}R_j}{\mathrm{d}\xi}\frac{\mathrm{d}R_i}{\mathrm{d}\xi} \tag{10}$$

$$k_{AB}(\xi) = -\sum_{i\in A}^{x,y,z}\sum_{j\in B\neq A}^{x,y,z} k_{ij}\frac{\mathrm{d}R_j}{\mathrm{d}\xi}\frac{\mathrm{d}R_i}{\mathrm{d}\xi} = k_{BA}(\xi) \tag{11}$$

The entire atomic contribution becomes

$$k_A(\xi) = k_{AA}(\xi) + \sum_{B\neq A}^{N} k_{AB}(\xi) \tag{12}$$

The reaction force constant k_ξ (eq 5) may then be divided into a sum of the pure atomic terms and the contribution from the bonds

DOI: 10.1021/acs.jpca.6b03408
J. Phys. Chem. A 2016, 120, 3780−3787

$$k_\xi = \sum_A^N k_{AA}(\xi) + 2\sum_A^N \sum_{B<A}^N k_{AB}(\xi) = k_\xi^{\text{atoms}} + k_\xi^{\text{bonds}} \tag{13}$$

Any group of atoms can be characterized accordingly

$$k_G(\xi) = \sum_{A\in G}^N k_A(\xi) = \sum_{A\in G}^N k_{AA}(\xi) + \sum_{A\in G}^N \sum_{B\neq A}^N k_{AB}(\xi) \tag{14}$$

3. RESULTS

The IRC energy profile has been reproduced by the standard procedure at the MP2 level using the 6-311++G(3df,3pd) basis set and the Gaussian 09 code.[35] The forces on atoms and the Cartesian force constants have been calculated separately using the geometry of the structures resulting on the IRC. The variable geometry of the reacting systems has been reflected by the calculated bond length. The effect of electronic flow is assessed by the atomic charges calculated in three typical computational schemes Mulliken (MUL), Hirschfeld (HIR), and natural orbital population analysis (NPA). Also, the Wiberg indices[36] for the formal bonds have been calculated for each configuration of reactants on the reaction path. The results are found in Figures 1 and 2 for the HF/CO and H/ONS systems, respectively.

Only the range ξ [−2,2] has been visualized in the diagrams (Figures 1 and 2); this is sufficient to reproduce all the major changes for the isomerization HONS (Figure 2). Inspection of the bond lengths and the Wiberg indices in Figure 2a reveals interesting effects. The reaction is viewed as a mere proton migration from O to S atoms (cf. graphic abstract), and this is clear from the bond distances H−O and H−S, with the O−N and N−S bonds being only slightly modified; however, the Wiberg indices for the latter two bonds change dramatically, indicating the change N−O to N═O as well as N═S to N−S. Surprisingly, the inflection points for the interchange between the H−O/H-S and O═N/N−S bonds do not coincide and remarkably precede the TS (W in Figure 2a). The proton migration is associated with the significant electron transfer that makes the charge on ONS group decreasing from $Q_{ONS} \cong -0.45$ to -0.1 by any of the approaches presented in Figure 2b. Apparently, this major reorganization of the density in the ONS moiety occurs with only minor change in its geometry.

For the HF/CO reaction, the C−F distance in the product molecule HCOF does not reach its equilibrium value at $\xi = 2$. Also, the C−F Wiberg index is not quite stabilized at this point. To a smaller extent the same is observed for the C−O bond parameters (R, W) (Figure 1a). It is important to note that atoms are not uniformly affected by the ongoing rearrangement, even in the reaction of as small entity as HFCO. Here again, the H−F bond vanishes before the TS is reached, while the diffuse W_{C-F} and W_{C-O} shapes indicate the inflection points to fall far beyond the TS, toward the configuration of the products. This finds interesting confirmation in the charge variation for the CO group (Figure 1 b): By any of the approaches presented, the charge goes through the maximum at $\xi = 0.5 \div 1.5$. This tends to suggest, a two-stage process occurring in this reaction: first−the H−C bond formation and second−the F−C bond formation, with appropriate adjustments in the density within CO group.

The first important information in the diagrams of the atomic (group) contributions to the reaction force in both reactions (Figures 3 and 4) is their uniform sign. The results of the IRC formalism are represented linearly, from one equilibrium

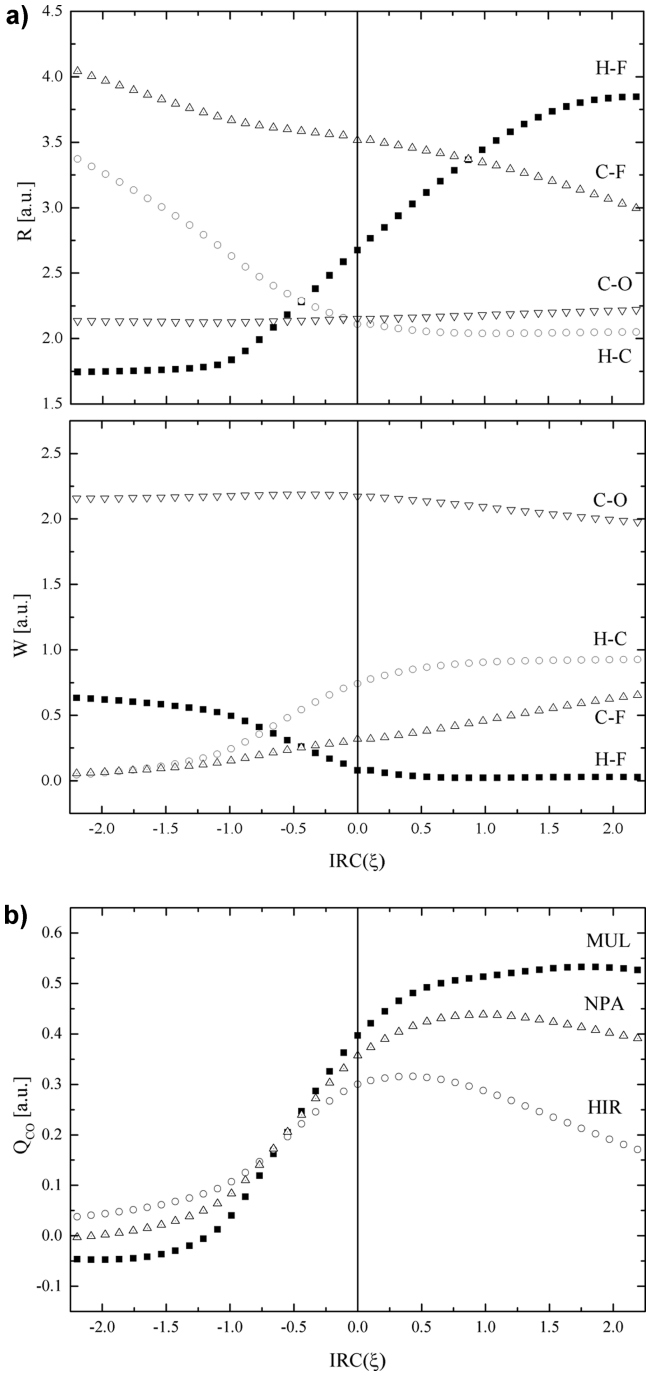

Figure 1. Variation of the geometry and electronic density indices in the reaction HF+CO → HCOF. (a) Bond lengths R and Wiberg bond indices W. (b) Charge on the CO group calculated in three typical approaches.

configuration (EQ1) through the transition state (TS) to the final configuration (EQ2); however, both EQ1 and EQ2 are equivalent with respect to TS. Starting at the TS, the product $F_A(\xi) = \mathbf{F}_A \cdot [d\mathbf{R}_A/d\xi] > 0$ (eq 6) would be positive for every atom, and so is the sum (F_ξ). In the linear representation, though, the first part of the reaction path requires an action against the force on each atom to have it shifted, hence $F_A(\xi) = \mathbf{F}_A \cdot [d\mathbf{R}_A/d\xi] < 0$.

The decomposition of the reaction force into atomic contributions for the HF/CO reaction is shown in Figure 3. CO and HF groups do not provide the same contribution to the

DOI: 10.1021/acs.jpca.6b03408
J. Phys. Chem. A 2016, 120, 3780−3787

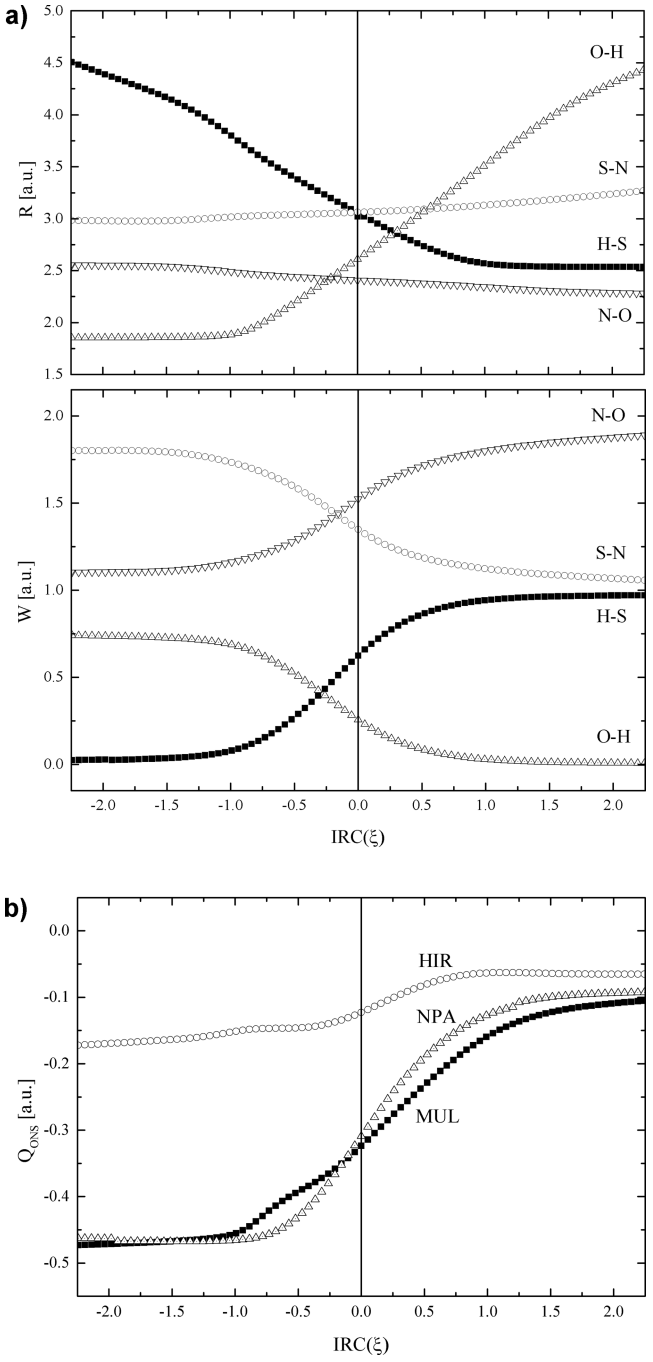

Figure 2. Variation of the geometry and electronic density indices in the reaction HONS → ONSH. (a) Bond lengths *R* and Wiberg bond indices *W*. (b) Charge on the SNO group calculated in three typical approaches.

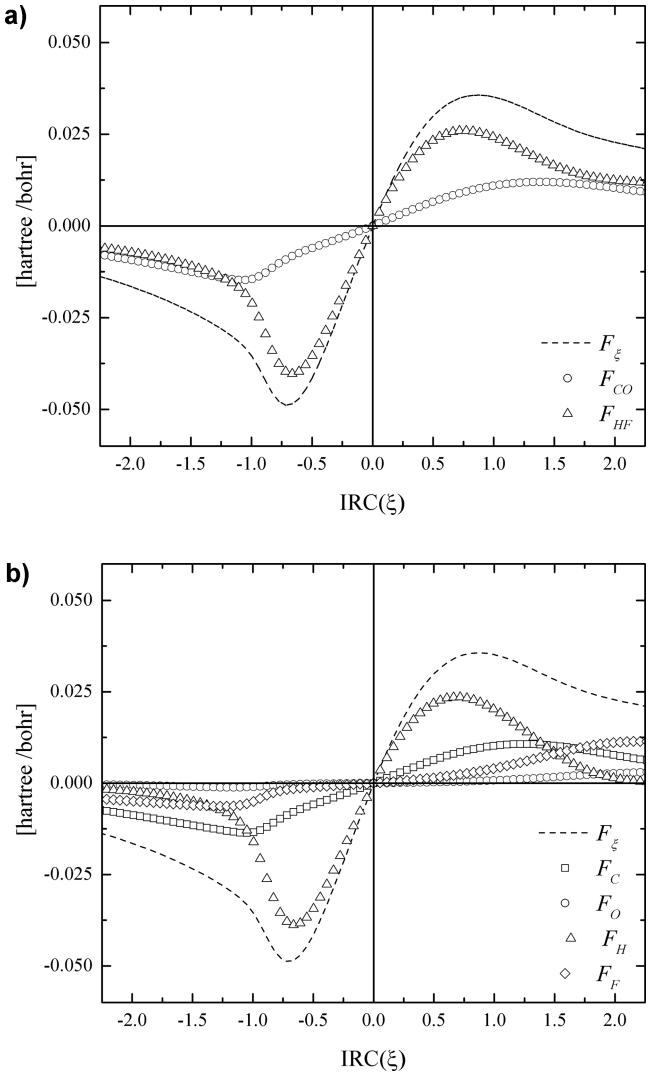

Figure 3. Variation of the reaction force in the reaction HF + CO → HCOF (dashed line) and the appropriate contributions to it: (a) from the reacting groups and (b) from individual atoms.

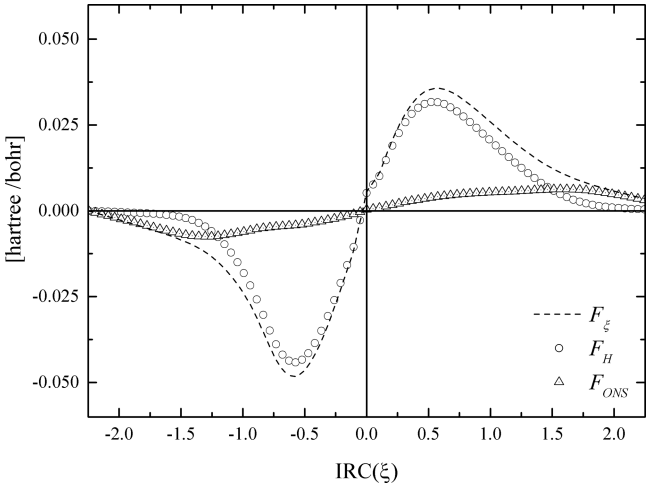

Figure 4. Variation of the reaction force (dashed line) and the appropriate contributions to it from the reacting groups in the reaction HONS → ONSH.

reaction force (Figure 3a), even though the reaction formally leads to the combination of the two parts. The hydrogen atom provides the major contribution to the reaction force in the HF/CO reaction (Figure 3b). This hints to much a different mechanism of the H and F attachment to the carbon atom, as the reaction affects evenly the hydrogen and fluorine atoms and the formal bond energies of the H−C and F−C bonds are close (bond dissociation enthalpies are ca. 99 and 116 kcal/mol, respectively). The structural data in Figure 1a do confirm that H−C bond and F−C formation bond formation are not simultaneous. The H−C bond is completed below $\xi = 1$, and the formation of the F−C is not completed even at $\xi = 2$ (*R*, *W*,

DOI: 10.1021/acs.jpca.6b03408
J. Phys. Chem. A 2016, 120, 3780−3787

Figure 1a). This could hardly be deduced from the classical integral F_ξ curve (dashed line) but is quite clear from the atomic contributions to the reaction force (Figure 3b). The F_F relationship does not reach a maximum even at $\xi = 2$; the same effect appears in Figure 3a only in the flat maximum on the F_{CO} curve near $\xi = 2$; indeed, the reaction gets completed only at $\xi = 3 \div 4$

The contributions to the reaction force in the H/ONS reaction have only been shown for the migrating proton and the ONS group in Figure 4. The reaction force is dominated by the proton displacement, followed by the second stage; the rearrangement within ONC group is still not stabilized (see above) when proton has reached its position. This is demonstrated by the flat increase in the F_{ONS} line, which barely reaches its maximum around $\xi = 1.6$.

The reaction force constant diagrams provide more analytical information. There is no a priori condition here concerning the sign of the product $[d\mathbf{F}_A/d\xi]\cdot[d\mathbf{R}_A/d\xi]$ (eq 6), and the diagrams reveal the variety of changes occurring at particular atoms (groups). The critical points are now very clearly represented by crossing the zero line by the curves (corresponding to the maxima in Figures 3 and 4), while the extremes in Figures 5 and 6 mark the inflection points in Figures 3 and 4. Changing the sign

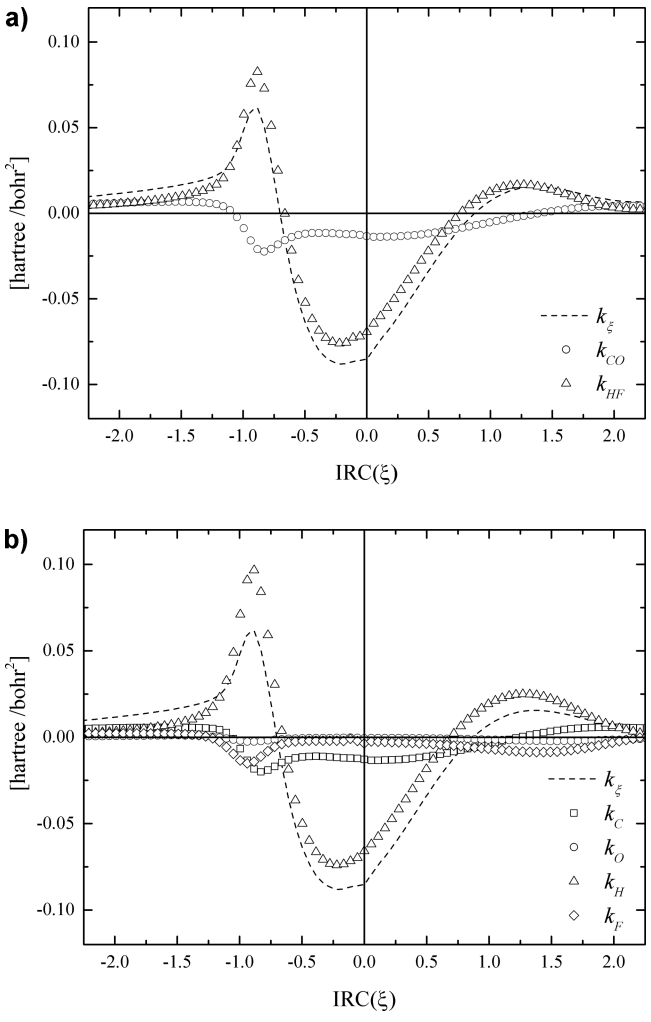

Figure 5. Variation of the reaction force constant (dashed line) in the reaction HF+CO → HCOF and the appropriate contributions to it in (a.u.): (a) from the reacting groups and (b) from individual atoms.

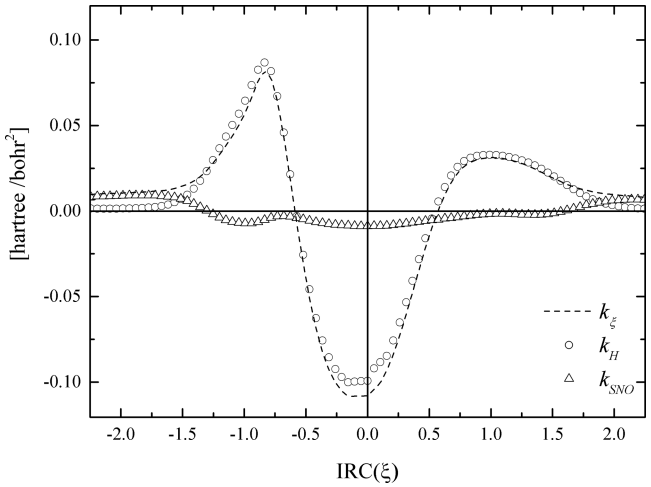

Figure 6. Variation of the reaction force constant (dashed line) and the appropriate contributions to it from the reacting groups in the reaction HONS → ONSH.

on k_H curve at ca. $\xi = -0.7$ results from the negative $d\mathbf{F}_H/d\xi$ derivative. It is clear in Figure 5 that the HF group contribution is dominated by H, while in the CO group the leading partner is C, suggesting that the hydrogen and carbon atoms provide the driving force for the reaction. Notably, the critical points ($k_\xi = 0$) for the HF and CO do not coincide.

In the H/ONS reaction the similar phenomenon is exposed in Figure 6: The minimum on k_ξ is an effect of hydrogen drift, which apparently is most significant even before the reaction reaches its TS. The ONS group seem to have little effect on the variation of k_ξ.

The common feature of the electron rich groups in both reaction (CO/F and ONS) is their largely negative contribution to k_ξ in wide range ($-1.2 < \xi < 1.5$). This should be confronted with the separation of the atomic and bond parts in the reaction force (eq 13) shown in Figure 7. Apparently, the k_G of big groups is dominated by the k_{ij} factors (eq 8); spectacular variation k_H for hydrogen moving around is a result of dominating $d\mathbf{R}_H/d\xi$. The role of electronic and geometrical factors is worth a more profound analysis provided in the next section.

There is a singularity on all k_ξ diagrams, as presented in Figures 5−7 (global value, dashed line): the minimum values of the reaction force constants do not match the TS, beyond the statistical errors of the method for both reactions, and appear at $\xi = -0.22$ and $\xi = -0.05$ for HF/CO and H/ONS reactions, respectively. Searching for the feasible explanation of this fact, the root-mean-square distance (RMSD[37]) parameter has been calculated for all structures along the IRC for the reactions (Figure 8). The calculated RMSD represents the root-mean-square of all interatomic distances in the reacting entity. The flat minima are observed on the RMSD(ξ) relationships; they are shifted off the TS in the same direction as on the k_ξ curves, although to somewhat more significant values ($\xi = -0.42$ and $\xi = -0.33$). Apparently, the nuclear interactions mark their role on the second derivative of the energy (k_ξ).

4. DISCUSSION AND CONCLUSIONS

The atomic contributions to the reaction force and reaction force constants reveal interesting informations about the involvement of atoms in various reaction stages. It becomes clear, that the transition state (TS) for the reaction represents just a maximum of the energy, while the chemistry is happening between the

DOI: 10.1021/acs.jpca.6b03408
J. Phys. Chem. A 2016, 120, 3780−3787

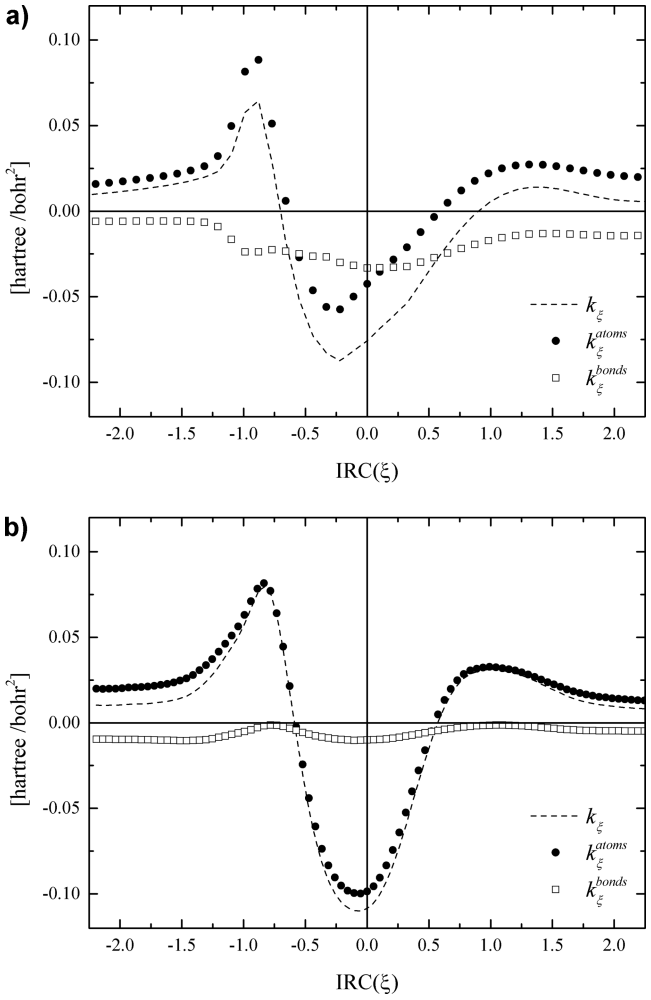

Figure 7. Variation of the atomic and bond contributions to the reaction force constants (dashed line) in eq 13: (a) reaction HF+CO → HCOF and (b) reaction HONS → ONSH.

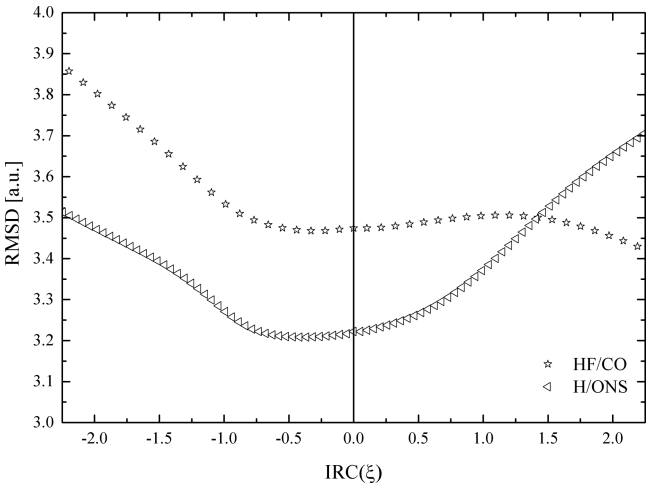

Figure 8. Root-mean-square distance (RMSD) of atomic positions calculated on the reaction path for the two reactions.

reacting atoms, step by step, with some bonds forming first (H−C in HF/CO) and some eventually being completed only at the very end (C−F) of the process. The global reaction force F_ξ and the reaction force constant k_ξ calculated on the IRC contain no more information than the energy curve itself, as they only demonstrate in detail its mathematical character. The pictures provided by the atomic components $F_A(\xi)$ and $k_A(\xi)$ reach a bit further: They unveil a role of an atom in the modification of the reacting structure. The pictures call for their interpretation in the chemical language: What is the sequence of changes in the geometry of the nuclei and in the electronic structure on each step on the reaction paths? The appropriate analysis is possible with a concept of Hellmann−Feynmann (H−F) forces acting on the nuclei.

H−F force on an atom can be reproduced by a sum of the electronic and nuclear contributions[16]

$$\mathbf{F}_A = -\left(\frac{\partial E_M}{\partial \mathbf{R}_A}\right)_N = \int \rho(\mathbf{r})\cdot\boldsymbol{\varepsilon}_A(\mathbf{r})\,\mathrm{d}\mathbf{r} + \mathbf{F}_A^{n-n} \tag{15}$$

Here $\rho(\mathbf{r})$ is electron density function, $\boldsymbol{\varepsilon}_A(\mathbf{r})$ is electric field of the nucleus A at given point $\mathbf{r}$, and $\mathbf{F}_A^{n-n}$ is the repulsion force from other nuclei acting on A.

$$\boldsymbol{\varepsilon}_A(\mathbf{r}) = -\frac{\mathrm{d}\nu(\mathbf{r})}{\mathrm{d}\mathbf{R}_A} \quad \text{where} \quad \nu(\mathbf{r}) = \frac{Z_A}{|\mathbf{R}_A - \mathbf{r}|} \tag{16}$$

$$\mathbf{F}_A^{n-n} = -\frac{\partial E^{n-n}}{\partial \mathbf{R}_A} = -Z_A\frac{\partial V_A^{n-n}}{\partial \mathbf{R}_A} \quad V_A^{n-n} = \sum_{B\neq A}^{\text{atoms}} \frac{Z_B}{|\mathbf{R}_A - \mathbf{R}_B|} \tag{17}$$

The force $\mathbf{F}_A$ is zero for every atom only in the equilibrium state; however, according to the Hohenberg−Kohn theorem,[22,38] the external potential $\nu(\mathbf{r})$ is determined by the stationary density function for whatever configuration of the nuclei. Hence, the density calculated for the variable structures observed along the IRC is being adapted to the changing geometry on each step, and variation of the $\mathbf{F}_A$ forces can be traced on the reaction path. Equation 15 combined with eqs 2 and 3 (the reaction force) and eqs 5 and 6 (the reaction force constant) opens a way to assess how the coupling of the electronic and geometrical changes is reflected in $\mathbf{F}_\xi$ and k_ξ.

The atomic contribution to the reaction force becomes

$$F_A(\xi) = \mathbf{F}_A\cdot\frac{\mathrm{d}\mathbf{R}_A}{\mathrm{d}\xi} = \left(\frac{\mathrm{d}\mathbf{R}_A}{\mathrm{d}\xi}\right)\cdot\int\rho(\mathbf{r})\cdot\boldsymbol{\varepsilon}_A(\mathbf{r})\,\mathrm{d}\mathbf{r} + \left(\frac{\mathrm{d}\mathbf{R}_A}{\mathrm{d}\xi}\right)\cdot\mathbf{F}_A^{n-n} \tag{18}$$

By summing over atoms (eq 2), applying eqs 16 and 17 and the chain rule, the global reaction force is obtained in the compact form, containing directly the electronic and nuclear contributions

$$F_\xi = -\int\rho(\mathbf{r})\cdot\frac{\mathrm{d}\nu(\mathbf{r})}{\mathrm{d}\xi}\,\mathrm{d}\mathbf{r} - \frac{\mathrm{d}E^{n-n}}{\mathrm{d}\xi} \tag{19}$$

The reaction force calculated on each step of the reaction path contains directly the effect of variable configuration of the nuclei on that step: once in the change of the external potential, $\mathrm{d}\nu(\mathbf{r})/\mathrm{d}\xi$, and also in the variation of the nuclear repulsion energy, $\mathrm{d}E^{n-n}/\mathrm{d}\xi$. Modifications of the density $\rho(\mathbf{r})$ are included only indirectly, by using the initial density of the step as a parameter: Even if no change in $\rho(\mathbf{r})$ occurred on a step, the nonzero reaction force would still result.

Equation 19 opens a way to understanding Figure 3 and 4. As it is clear from the calculated RMS distances for the structures under study (Figure 8), the nuclear energy E^{n-n} stays nearly constant in the central part of the reaction path. The reaction force in HF/CO in the range $(-0.7 < \xi < 1)$ is dominated by the electronic term (eq 19), and it is the HF moiety that contributes

DOI: 10.1021/acs.jpca.6b03408
J. Phys. Chem. A 2016, 120, 3780−3787

most (Figure 3), by approaching the carbon atom (Figure 1a: R); losing connection inside the HF bond appears to be the leading electronic reorganization that occurs. The reaction force in H/ONS is by large dominated by the moving proton (Figure 4), and this is the increasing H−S interaction that makes the show, judging from the variable H−S and S−N distances (Figure 1b: R) in the central range of the reaction (flat RMSD: $-0.7 < \xi < 0.5$, Figure 8).

The reaction force constant k_ξ allows for similar analysis. The derivative of eq 15 gives

$$\frac{\mathrm{d}\mathbf{F}_A}{\mathrm{d}\xi} = \int \frac{\mathrm{d}\rho(\mathbf{r})}{\mathrm{d}\xi}\cdot\boldsymbol{\varepsilon}_A(\mathbf{r})\mathrm{d}\mathbf{r} + \int \rho(\mathbf{r})\cdot\frac{\mathrm{d}\boldsymbol{\varepsilon}_A(\mathbf{r})}{\mathrm{d}\xi}\mathrm{d}\mathbf{r} + \frac{\mathrm{d}\mathbf{F}_A^{n-n}}{\mathrm{d}\xi} \tag{20}$$

This equation brings together factors variable when the reaction occurs: position of the nuclei and the electron density. First, it is an enlightening exercise to prove that the second term on the right side is immaterial. We transform the first term by using the identity fundamental for the conceptual DFT formalism $\rho(\mathbf{r}) = \delta E^{el}/\delta v(\mathbf{r})$, where $E^{el} = E_M - E^{n-n}$ (the definition given by eq 16 is also instrumental)

$$\begin{aligned}\int \frac{\mathrm{d}\rho(\mathbf{r})}{\mathrm{d}\xi}\cdot\boldsymbol{\varepsilon}_A(\mathbf{r})\mathrm{d}\mathbf{r} &= -\int \frac{\mathrm{d}\rho(\mathbf{r})}{\mathrm{d}\xi}\cdot\frac{\partial v(\mathbf{r})}{\partial \mathbf{R}_A}\mathrm{d}\mathbf{r}\\ &= -\int \frac{\mathrm{d}}{\mathrm{d}\xi}\left(\frac{\delta E^{el}}{\delta v(\mathbf{r})}\right)\cdot\frac{\partial v(\mathbf{r})}{\partial \mathbf{R}_A}\mathrm{d}\mathbf{r} = -\int \frac{\delta}{\delta v(\mathbf{r})}\left(\frac{\mathrm{d}E^{el}}{\mathrm{d}\xi}\right)\cdot\frac{\partial v(\mathbf{r})}{\partial \mathbf{R}_A}\mathrm{d}\mathbf{r}\\ &= -\frac{\partial}{\partial \mathbf{R}_A}\left(\frac{\mathrm{d}E^{el}}{\mathrm{d}\xi}\right) = \frac{\mathrm{d}\mathbf{F}_A}{\mathrm{d}\xi} - \frac{\mathrm{d}\mathbf{F}_A^{n-n}}{\mathrm{d}\xi}\end{aligned} \tag{21}$$

This proves vanishing the second term in eq 20. The reaction force constant (eqs 5 and 6) is now decomposed into the electronic and nuclear contributions

$$k_\xi = -\sum_A^N \frac{\mathrm{d}\mathbf{F}_A}{\mathrm{d}\xi}\frac{d\mathbf{R}_A}{\mathrm{d}\xi} = \sum_A^N \frac{\mathrm{d}\mathbf{R}_A}{d\xi}\int \frac{\mathrm{d}\rho(\mathbf{r})}{\mathrm{d}\xi}\cdot\frac{\partial v(\mathbf{r})}{\partial \mathbf{R}_A}\mathrm{d}\mathbf{r} - \sum_A^N \frac{\mathrm{d}\mathbf{F}_A^{n-n}}{\mathrm{d}\xi}\frac{d\mathbf{R}_A}{\mathrm{d}\xi} \tag{22}$$

Hence, by applying the method tested with eq 19, the reaction force constant is represented by the compact form

$$k_\xi = \int \frac{\mathrm{d}\rho(\mathbf{r})}{\mathrm{d}\xi}\cdot\frac{\nu(\mathbf{r})}{\mathrm{d}\xi}\,\mathrm{d}\mathbf{r} + \frac{\mathrm{d}^2E^{n-n}}{\mathrm{d}\xi^2} \tag{23}$$

Here again the electronic and nuclear contributions to the reaction force constant are fully exposed. The variable density is now the crucial component of the electronic part in k_ξ. The characteristic feature of k_ξ is its large and negative value in the central region and the positive side wings. Given the approximately flat E^{n-n} in the central region, eq 23 hints to the electron energy that must be responsible for the energy maximum at the TS.

The general conclusion of this work is corroborating the intuitive guess that the central part of the reaction path is largely dominated by the electronic reorganization. Other expectations have been proved to be too far reaching, although the geometrical configuration of the system is not quite stationary in the central region around the TS; on the contrary, the electronic reorganization happens due to the displacement of selected initiators of the process, like H−F group (in HF/CO) and H (in H/ONS). Discovering the entities active in such a way may be valuable in practice for the reaction run. The electronic reorganization on the reaction path is by no means limited to the central region. It may continue as an aftermath in regions that did not participate in the main event (CO in HF/CO), and reaching the equilibrium may require astonishingly many additional steps on the IRC. This finding calls for the direct analysis of the nuclear and electronic energies as well as their derivatives along the reaction path. The challenging problem for these studies is going beyond the IRC format, that is, tracing the reaction started from an arbitrary configuration of the nuclei, thus with the defined nuclear repulsion energy, resulting from the impact of the reacting entities.[39]

AUTHOR INFORMATION

Corresponding Author

*E-mail: ludwik.komorowski@pwr.edu.pl. Tel: +48 713 203 937.

Notes

The authors declare no competing financial interest.

ACKNOWLEDGMENTS

The work was financed by a statutory activity subsidy from the Polish Ministry of Science and Higher Education for the Faculty of Chemistry of Wrocław University of Technology, ref. no. S50013/K0301. The use of resources of Wrocław Center for Networking and Supercomputing (WCSS) is gratefully acknowledged. We are indebted to a referee for the much enlightening remarks.

REFERENCES

(1) Toro-Labbé, A. Characterization of Chemical Reactions from the Profile of Energy, Chemical Potential, and Hardness. *J. Phys. Chem. A* **1999**, *103*, 4398−4403.

(2) Herrera, B.; Toro-Labbé, A. The Role of Reaction Force and Chemical Potential in Characterizing the Mechanism of Double Proton Transfer in the Adenine-Uracil Complex. *J. Phys. Chem. A* **2007**, *111*, 5921−5926.

(3) Echegaray, E.; Toro-Labbé, A. Reaction Electronic Flux: A New Concept to Get Insight into Reaction Mechanism. Study of Model Symmetric Nucleophilic Substitutions. *J. Phys. Chem. A* **2008**, *112*, 11801−11807.

(4) Flores-Morales, P.; Gutiérrez-Oliva, S.; Silva, E.; Toro-Labbé, A. The Reaction Electronic Flux: A New Descriptor of the Electronic Activity Taking Place During a Chemical Reaction. Application to the Characterization of the Mechanism of the Schiff's Base Formation in the Maillard Reaction. *J. Mol. Struct.: THEOCHEM* **2010**, *943*, 121−126.

(5) Cerón, M. L.; Echegaray, E.; Gutiérrez-Oliva, S.; Herrera, B.; Toro-Labbé, A. The Reaction Electronic Flux in Chemical Reactions. *Sci. China: Chem.* **2011**, *54*, 1982−1988.

(6) Jaque, P.; Toro-Labbé, A.; Politzer, P.; Geerlings, P. Reaction Force Constant and Projected Force Constants of Vibrational Modes Along the Path of an Intramolecular Proton Transfer Reaction. *Chem. Phys. Lett.* **2008**, *456*, 135−140.

(7) Politzer, P.; Murray, J. S. The Position Dependent Force Constant in Bond Dissociation/Formation. *Collect. Czech. Chem. Commun.* **2008**, *73*, 822−830.

(8) Yepes, D.; Murray, J. S.; Politzer, P.; Jaque, P. The Reaction Force Constant: An Indicator of the Synchronicity in Double Proton Transfer Reactions. *Phys. Chem. Chem. Phys.* **2012**, *14*, 11125−11134.

(9) Yepes, D.; Donoso-Tauda, O.; Perez, P.; Murray, J. S.; Politzer, P.; Jaque, P. The Reaction Force Constant as an Indicator of Synchronicity/Nonsynchronicity in [4 + 2] Cycloaddition Processes. *Phys. Chem. Chem. Phys.* **2013**, *15*, 7311−7320.

(10) Toro-Labbé, A.; Gutiérrez-Oliva, S.; Politzer, P.; Murray, J. S. Reaction Force: A Rigorously Defined Approach to Analyzing Chemical and Physical Processes. In *Chemical Reactivity Theory. A Density Functional Viewpoint*; Chattaraj, P. K., Ed.; CRC Press, Taylor & Francis Group: Boca Raton, FL, 2009.

(11) Politzer, P.; Toro-Labbé, A.; Gutiérrez-Oliva, S.; Murray, J. S. Perspectives on the Reaction Force. *Adv. Quantum Chem.* **2012**, *64*, 189−209.

DOI: 10.1021/acs.jpca.6b03408
J. Phys. Chem. A 2016, 120, 3780−3787

(12) Yepes, D.; Murray, J. S.; Santos, J. C.; Toro-Labbe, A.; Politzer, P.; Jaque, P. Fine Structure in the Transition Region: Reaction Force Analyses of Water-Assisted Proton Ttransfer. *J. Mol. Model.* **2013**, *19*, 2689−2697.
(13) Inostroza-Rivera, R.; Yahia-Ouahmed, M.; Tognetti, V.; Joubert, L.; Herrera, B.; Toro- Labbé, A. Atomic Decomposition of Conceptual DFT Descriptors: Application to Proton Transfer Reactions. *Phys. Chem. Chem. Phys.* **2015**, *17*, 17797−17808.
(14) Pendas, A. M.; Blanco, M. A.; Francisco, E. Two Electron Integrations in the Quantum Theory of Atoms in Molecules. *J. Chem. Phys.* **2004**, *120*, 4581−4592.
(15) Vöhringer-Martinez, E.; Toro- Labbé, A. Understanding the Physics and Chemistry of Reaction Mechanisms from Atomic Contributions: A Reaction Force Perspective. *J. Phys. Chem. A* **2012**, *116*, 7419−7423.
(16) Ordon, P.; Komorowski, L. Nuclear Reactivity and Nuclear Stiffness in Density Functional Theory. *Chem. Phys. Lett.* **1998**, *292*, 22−27.
(17) Ordon, P. The Role of Molecular Deformations for the Chemical DFT Indices, Ph.D. Thesis, Wrocław University of Technology: Wrocław, Poland, 2003.
(18) Komorowski, L.; Ordon, P. Vibrational Softening of Diatomic Molecules. *Theor. Chem. Acc.* **2001**, *105*, 338−344.
(19) Komorowski, L.; Ordon, P. Fluctuations in Electronegativity and Global Hardness Induced by Molecular Vibrations. *J. Mol. Struct.: THEOCHEM* **2003**, *630*, 25−32.
(20) Komorowski, L.; Ordon, P. DFT Analysis of Fluctuations in Electronegativity and Hardness of a Molecular Oscillator. *Int. J. Quantum Chem.* **2003**, *91*, 398−403.
(21) Ordon, P.; Komorowski, L. DFT Energy Derivatives and Their Renormalization in Molecular Vibrations. *Int. J. Quantum Chem.* **2005**, *101*, 703−713.
(22) Hohenberg, P.; Kohn, W. Inhomogeneous Electron Gas. *Phys. Rev.* **1964**, *136*, 8864−8871.
(23) Ordon, P.; Tachibana, A. Use of Nuclear Stiffness in Search for a Maximum Hardness Principle and for the Softest States Along the Chemical Reaction Path: A New Formula for the Energy Third Derivative γ. *J. Chem. Phys.* **2007**, *126*, 234115.
(24) Ordon, P.; Tachibana, A. Nuclear Reactivity Indices Within Regional Density Functional Theory. *J. Mol. Model.* **2005**, *11*, 312−316.
(25) Jędrzejewski, M.; Ordon, P.; Komorowski, L. Variation of the Electronic Dipole Polarizability on the Reaction Path. *J. Mol. Model.* **2013**, *19*, 4203−4207.
(26) Herrera, B.; Toro- Labbé, A. Theoretical Study of the HXNY→XNYH (X,Y = O,S) Intramolecular Proton Transfer Reactions. *J. Phys. Chem. A* **2004**, *108*, 1830−1836.
(27) Gutiérrez-Oliva, S.; Herrera, B.; Toro-Labbé, A.; Chermette, H. On the Mechanism of Hydrogen Transfer in the HSCH(O)→(S)-CHOH and HSNO→SNOH Reactions. *J. Phys. Chem. A* **2005**, *109*, 1748−1751.
(28) Morell, C.; Herrera, B.; Gutiérrez-Oliva, S.; Cerón, M. L.; Grand, A.; Toro- Labbé, A. Relation Between Differential Scales of Electrophilicity: Are the Scales Consistent Along a Chemical Reaction. *J. Phys. Chem. A* **2012**, *116*, 7074−7081.
(29) Yepes, D.; Murray, J. S.; Santos, J. C.; Toro- Labbé, A.; Politzer, P.; Jaque, P. Fine Structure in the Transition Region: Reaction Force Analyses of Water-Assisted Proton Transfer. *J. Mol. Model.* **2013**, *19*, 2689−2697.
(30) Piela, L. Section 14.3: Intrinsic Reaction Coordinate (IRC) or Statics. In *Ideas of Quantum Chemistry*; Elsevier: Amsterdam, The Netherlands, 2007.
(31) Martinez, J.; Toro- Labbé, A. The reaction force. A Scalar Property to Characterize Reaction Mechanisms. *J. Math. Chem.* **2009**, *45*, 911−927.
(32) Toro-Labbé, A.; Gutiérrez-Oliva, S.; Murray, J. S.; Politzer, P. A new Perspective on Chemical and Physical Processes: The Reaction Force. *Mol. Phys.* **2007**, *105*, 2619−2625.
(33) Toro-Labbé, A.; Gutiérrez-Oliva, S.; Murray, J. S.; Politzer, P. *J. Mol. Model.* **2009**, *15*, 707−710.
(34) Wilson, E. B., Jr; Decius, J. C.; Cross, P. C. *Molecular Vibrations*; Dover Publications: New York, 1980.
(35) Frisch, M. J.; Trucks, G. W.; Schlegel, H. B.; Scuseria, G. E.; Robb, M. A.; Cheeseman, J. R.; Scalmani, G.; Barone, V.; Mennucci, B.; Petersson, G. A.; et al. *Gaussian 09*, Revision A.02; Gaussian, Inc.: Wallingford, CT, 2009.
(36) Mayer, I. Bond Orders and Valence Indices: A Personal Account. *J. Comput. Chem.* **2007**, *28*, 204−221.
(37) Carugo, O.; Pongor, S. A normalized root-mean-square distance for comparing protein three-dimensional structures. *Protein Sci.* **2001**, *10*, 1470−1473.
(38) Parr, R. G.; Yang, W. *Density-Functional Theory of Atoms and Molecules*; Oxford University Press: Oxford, U.K., 1989.
(39) Luty, T.; Ordon, P.; Eckhardt, C. J. A model for mechanochemical transformations: Applications to molecular hardness, instabilities, and shock initiation of reaction. *J. Chem. Phys.* **2002**, *117*, 1775−1785.

DOI: 10.1021/acs.jpca.6b03408
J. Phys. Chem. A 2016, 120, 3780−3787